PRECISE AERONAUTICAL GROUND BASED NAVIGATION USING LDACS1

N. Schneckenburger, D. Shutin, M. Schnell, German Aerospace Center (DLR), Germany

Abstract

In order to cope with the increasing demand for communication capacity in the aeronautical sector, the Future Communications Infrastructure is currently being developed. For air-ground communications two candidates are considered as the new L-band digital aeronautical communication system. In this paper, the idea of using one of these systems, namely LDACS1, as navigation aid is presented. Compared to satellite based navigation systems, LDACS1 exhibits a significantly lower vulnerability to intentional or unintentional interference. This is due to its larger received power.

Despite LDACS1's general fitness to perform positioning, so far no precise ranging algorithm has been adopted. The standard LDACS1 synchronization procedure offers a simple ranging possibility, however, with restricted accuracy. Therefore, in this paper two newly adopted algorithms for determining precise range estimates between the aircraft and the ground station are presented. This also includes an assessment of the theoretical and currently achievable ranging precision. It is shown that the two algorithms offer a superior performance to the previously employed synchronization procedure.

Introduction

To enable the modernization of Air-Traffic Management (ATM) as currently pursued by NextGen [1] in the US and SESAR in Europe [2], new and efficient communication, navigation, and surveillance technologies are required.

For communications, a common understanding within ICAO has been reached that a single data link technology is not capable of covering the communication needs for all phases of flight. Therefore, the Future Communications Infrastructure (FCI) has been developed. It comprises a set of data link technologies for aeronautical communications [3]: a future satellite-based communications system developed within the ESA Iris program, AeroMACS (Aeronautical Mobile Airport Communications System) for the airport, and the new L-band Digital Aeronautical Communication System (LDACS) for air-ground communications. For LDACS two candidate systems, LDACS1 and LDACS2, are under consideration. LDACS1 employs a frequency division duplex broadband transmission using Orthogonal Frequency-Division Multiplexing (OFDM). In contrast, LDACS2 is a narrowband single-carrier system employing time-division duplex. The new L-band system is mainly to be used for communications between pilots and air-traffic controllers. Additionally, the system is foreseen for supplemental data services, like the transmission of weather information or general airline data.

In the last few years a rising demand for precise navigation with a high quality of service has been observed. Improving the quality of navigation in the aeronautical sector allows for better routing of aircraft as well as for more efficient routes during approach, landing, and take-off. In order to fulfill these requirements, ICAO recommends an increased use of Global Navigation Satellite System (GNSS) technologies. Currently, GNSS is mostly used for en-route but in the future the use of GNSS is also planned for approach, landing, and take-off. To achieve the required navigation performance in terms of precision, continuity, and integrity, augmentation systems are used to assist GNSS, e.g. SBAS (Satellite Based Augmentation System), A-RAIM (Advanced Receiver Autonomous Integrity Monitoring) or GBAS (Ground Based Augmentation System). This way, GNSS based navigation is expected to cover even CAT III landings in the future.

Using GNSS in safety sensitive environments like civil aviation has major drawbacks. First, if one or several satellites fail, the position may not be calculated correctly. Large undetected errors might occur if no integrity information is present. This problem can be avoided by using one of the augmentation systems mentioned above. Second, the low received signal power is another serious problem: GNSS signals can easily be jammed either intentionally or unintentionally by terrestrial systems. An example of how easily GNSS signals might be jammed demonstrates the GBAS station at Newark

Liberty International Airport. GPS jammers used by truck drivers on the nearby highway caused the GBAS station to continuously shut itself down, ceasing its intended operation[1].

Because of these disadvantages of GNSS systems, the required availability and quality of service cannot itself be guaranteed. Therefore, an alternative system, known as alternative positioning, navigation, and timing (APNT), has to be available in case of GNSS failure. A possible approach is to increase the density of the distance measurement equipment (DME) stations on ground and perform multilateration with the DME signals for navigation. This, however, exhibits major drawbacks. First, a costly extension of the infrastructure is required. Second, this approach might have a severe impact on the operation of any future L-band communication system. Setting up additional DME stations would intensify the spectrum usage in L-band by navigation means making it much more complicated to find sufficient spectrum resources to cover the growing communications demand. A sustainable use of the L-band for communications and navigation as recommended by ICAO might be hard to achieve.

To enable sustainable use of L-band spectrum resources, a different approach is proposed: the use of the communication system LDACS1 for navigation. This way, the concept of using signals-of-opportunity is employed leading to efficient and sustainable usage of L-band spectrum resources. In [4], the general approach of positioning using a wireless network has been proposed, and in [5], it has been shown that positioning with an OFDM system is possible with high accuracy. As for LDACS1, which is also an OFDM system, only small adjustments are necessary for an integration of a navigation functionality. First theoretical results of the expected performance has been given in [6].

In a pseudolite approach for navigation with four LDACS1 ground stations the three coordinates as well as the clock offset can be computed. The range between the aircraft and the ground station may be calculated using a straightforward scheme. A coarse synchronization is computed using the conventional OFDM synchronization algorithm which is then followed by a finer timing determination using correlation analysis with transmitted sequences. In a later stage, the computation of the ranges allows positioning with LDACS1. Note, the ground infrastructure for this APNT approach is mainly deployed through the implementation of the LDACS1 system and, therefore, additional costs for APNT are kept at a minimum.

The main focus of this paper is the determination of the ranges between the aircraft and the ground stations. So far only the standard LDACS1 synchronization procedure has been considered for the range measurements. However, this straight forward approach exhibits a rather restricted accuracy. Therefore, in this paper two new algorithms are proposed in order to perform the ranging with a higher precision.

The paper is organized as follows: First a brief overview to the LDACS1 system is given. This description mainly focuses on the physical layer. The following section deals with the theoretical background of ranging with LDACS1. Firstly, this includes a short derivation of the optimum performance bound. Secondly, the different algorithms discussed in this paper are described. This includes the standard LDACS1 synchronization procedure as well as more sophisticated algorithms, explicitly used for improving the ranging accuracy. In the following section, the simulation results for the different algorithms are presented. In the end conclusions are drawn as well as an outlook on the research to be conducted in the future is given.

LDACS1 System Overview

To allow for a better understanding of the functional principles of LDACS1, first a brief summary about the fundamental parameters of LDACS1 is given. For further details on LDACS1 the reader is referred to [7].

LDACS1 is a cellular system based on a network of ground stations (GS), all synchronized in terms of time. The communication between a GS and an aircraft, here referred to as airborne station (AS), employs OFDM. Two different modes exist; the forward link (FL) incorporates transmissions from

[1] The GPS jammers are used by truck drivers to disable the tracking devices installed by their companies. GPS jammers, also often referred to as personal privacy devices, are inexpensive and can be purchased easily from the internet.

the GS to the AS while the reverse link (RL) is employed in the opposite direction.

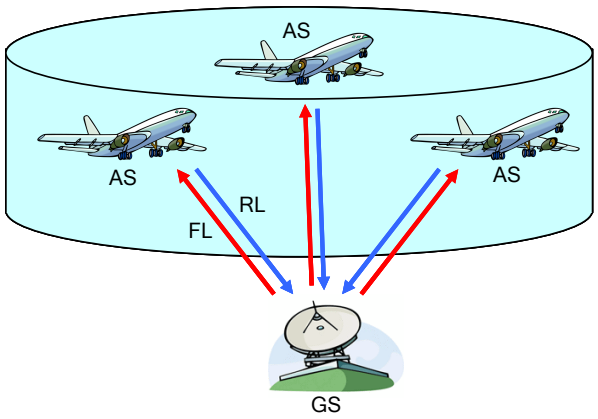

Figure 1. LDACS1 Network Topology

The FL signal from a GS is always transmitted as a time continuous broadcast which can be received by all AS within the radio horizon. Hence, it offers a perfect possibility for aircraft to synchronize and perform ranging to this GS. Ranging to the GS the AS is currently assigned to is straight forward since the AS is already synchronized to this GS for communication. Ranging to other GS requires additional, but limited efforts as described later in this section.

In the RL a combined Orthogonal Frequency-Division Multiple-Access (OFDMA) and Time-Division Multiple-Access (TDMA) approach is employed. A scheduler in the GS dynamically allocates on request certain blocks of sub-carriers for a certain time to an AS. This is done according to the specific traffic requirements of that AS.

LDACS1 shall be deployed in L-band (960-1164 MHz). The preferred deployment scenario is the inlay scenario where LDACS1 channels are put in between successive DME channels with an offset of 500 kHz with respect to the DME center frequencies. The proposed frequency bands for the inlay scenario are 985.5 - 1008.5 MHz for FL and 1048.5 - 1071.5 MHz for RL. FL and RL channels are assigned pairwise with a frequency spacing of 63 MHz. To enable coexistence between LDACS1 and other L-band systems, especially DME, mutual inference is minimized. To avoid excessive interference towards DME systems, means for reduction of out-of-band radiation are incorporated in the LDACS1 specification allowing to achieve a strict spectral mask. For mitigating the interference from DME and other L-band systems at the LDACS1 receiver several interference mitigation algorithms have been developed [8]. These algorithms guarantee reliable operation of LDACS1 even under worst-case assumptions for L-band interference. The results for first L-band compatibility measurements have been presented in [9].

The nominal size of the fast Fourier transform (FFT) used for the OFDM signal generation in LDACS1 is 64. The nominal FFT bandwidth is $\Delta f_{\text{nom}} = 625$ kHz resulting in a sub-carrier spacing of $\Delta f_{\text{s}} \approx 9.77$ kHz. However, only 50 sub-carriers are used for the actual data transmission and 14 are left empty – seven guard sub-carriers on the left, six guard sub-carriers on the right side, and the DC (direct current) sub-carrier. This leads to an effective bandwidth of $\Delta f_{\text{useful}} \approx 498$ kHz.

Each OFDM symbol with the useful symbol duration of $t_{\text{useful}} = 102.4$ µs (64 samples) is extended into a cyclic prefix (CP) of length $t_{\text{cp}} = 4.8$ µs (3 samples). Additionally, a raised cosine windowing function is applied to each OFDM symbol reducing its out-of-band radiation considerably. This adds another $t_{\text{win}} = 12.8$ µs (8 samples) on each side of an OFDM symbol. Due to the overlapping of the windowing function between consecutive symbols the overall symbol duration is $t_{\text{symbol}} = 120$ µs (75 samples). The overall CP and windowing overhead is about 15 %.

As for any modern communication system a high number of different combinations of coding and modulation settings exist. Using those, the transmission can be continuously adapted to the current channel and interference conditions as well as user requirements. In LDACS1 the coding consists of a Reed-Solomon (RS) code concatenated with a convolutional coding scheme. The overall coding rate can be varied. As modulation alphabets, QPSK, 16QAM and 64QAM are available.

Framing

The frame structure used in LDACS1 is of great importance for the quality of ranging. Since this paper deals with ranging using the FL signal, only the structure of the frames transmitted by the GS is covered here.

The GS transmit signal is organized in the structure shown in Figure 2. The largest entity is a super frame (SF) of length 240 ms. A SF consists of one broadcast (BC) and 4 multi frames (MF). While the MF employs the transmission of user specific data, the BC frame transmits signaling information relevant for all active AS in the cell. However the data transmitted on the BC is neither safety nor time critical. Thus, it is fully sufficient to decode the BC of the current GS only every few seconds. Therefore, the BC window is a perfect opportunity to tune the frequency to a different GS and perform ranging to that GS. Although it is possible to also use the data frames within the MF for ranging, we only consider ranging based on the BC frames which is a kind of worst case assumption.

One BC frame consists of 3 sub-frames. The BC1/2/3, shown in Figure 3. While the entire BC1 and BC3 are mainly used for power control to allow the receiving amplifier to adjust to the correct power level, the actual information is transmitted within the BC2. Each BC sub-frame consists of two OFDM symbols reserved for a synchronization sequence. This synchronization sequence is known both at the receiver and transmitter. More information on the synchronization symbols and the algorithm is given in a later section. The number of OFDM data symbols depends on the sub-frame type, 13 for the BC1/3 and 24 for the BC2. This leads to an overall sub-frame duration of 1.8 and 3.12 ms for the BC1/3 and BC2, respectively. The reason for the pilots being arranged in an irregular pattern rather than a regular is, that this constellation has proven to show a smaller vulnerability towards pulse like interference, as experienced by DME transmissions.

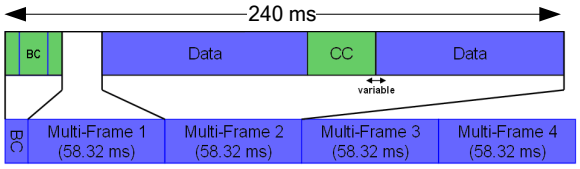

Figure 2. FL Super-Frame Structure of LDACS1

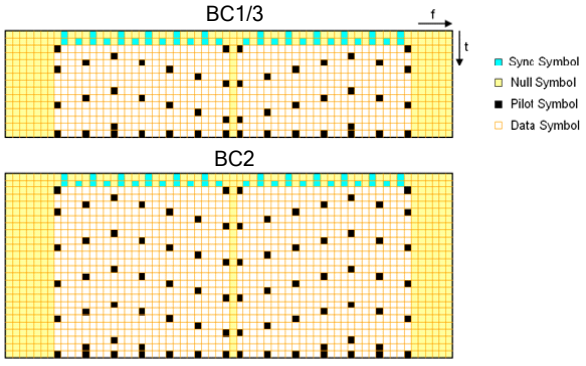

Figure 3. BC Frame Structure

Theoretical Background on the Employed Algorithms

In this section, the theoretical background necessary for ranging using the OFDM system LDACS1 and the used algorithms are described. First, the optimum bound for detecting a time-shift of an OFDM signal, described by the Cramer-Rao lower bound (CRLB), is given.

In order to use LDACS1 for reliable data communications, both the start of a frame and the start of the OFDM symbols have to be estimated. This is done applying a Schmidl-Cox like algorithm on the synchronization sequences of the LDACS1 signal [11]. Although the achieved synchronization accuracy is sufficient for decoding the data, the performance of this algorithm is rather poor. This is mainly caused be the short correlation length and the OFDM signal's low sampling rate of 0.625 Msample/s. Despite the low accuracy, this synchronization algorithm can be used as a good starting point for more sophisticated algorithms.

In order to increase the accuracy for the range estimates additional algorithms have to be applied. Therefore, two different approaches are studied: one approach performs range estimation in the time domain using ideal low pass interpolation; the other approach analyzes the phase of the received signal in the frequency domain.

Cramer-Rao Lower Bound for Ranging With OFDM

Assume a time discrete OFDM transmit signal of length K, shifted by the unknown time constant τ, given as

$$s[\mathrm{k}-\tau] = \frac{1}{\sqrt{N}} \sum_{n=\left\lfloor -\frac{N-1}{2} \right\rfloor}^{\left\lfloor \frac{N-1}{2} \right\rfloor} S[n] e^{j2\pi n f_{sc}(\mathrm{k}-\tau)}$$

with N denoting the number of sub-carriers, $S[n]$ the complex modulation symbol on carrier n and f_{sc} the sub-carrier spacing. To the transmit signal $s[k]$ zero-mean Gaussian noise with the variance σ^2 is added generating the receive signal $y[k]$

$$y[k] = s[k-\tau] + n[k], \;\; n[k] \sim \mathcal{N}(0, \sigma^2).$$

The goal is to estimate the unknown shift τ from the received signal $y[k]$. When trying to evaluate the performance of an arbitrary algorithm, always some kind of comparison is needed. Probably the best solution is, if the algorithm studied, can be compared with the theoretically best solution of the problem, the optimum algorithm.

For the problem described above, the performance, i.e. the accuracy, of the optimum algorithm can be calculated using the Cramer-Rao lower bound (CRLB) [10]. Applied to ranging with LDACS1, the CRLB describes the variance of the estimate $\hat{\tau}$ trying to estimate the unknown shift τ of the transmit signal $s[k-\tau]$ by analyzing the receive signal $y[k]$. The CRLB is given as

$$VAR\{\hat{\tau}\} \geq \frac{1}{E\{|\frac{d}{d\alpha} \ln p(\boldsymbol{y}|\tau)\,|^2\}}$$

with E denoting the expected value and $p(y|\tau)$ the parameterized likelihood function, describing how the receive signal $\boldsymbol{y} = [y[1], \dots, y[K]]^T$ depends on the parameter τ to be estimated. The likelihood function of the transmit signal with additive Gaussian noise is given as

$$\begin{aligned} p(\boldsymbol{y}|\tau) &= \prod_{k=0}^{K} p(y[k]|\tau) \\ &= (2\pi\sigma^2)^{-\frac{K}{2}} \mathrm{e}^{-\frac{1}{2\sigma^2}\sum_{k=0}^{K}(s[\mathrm{k}-\tau]-y[k])^2} \end{aligned}$$

Using the formulas above, the minimum variance for the estimation of τ from $y[k]$ can be calculated as

$$VAR\{\hat{\tau}\} \geq \frac{\sigma^2}{\sum_{k=1}^{K}(\frac{d}{d\tau} s[\mathrm{k}-\tau])^2}$$

$$\geq \frac{\sigma^2}{8\pi^2 f_{sc}^2 \sum_{n=\left\lfloor -\frac{N-1}{2} \right\rfloor}^{\left\lfloor \frac{N-1}{2} \right\rfloor} n^2 |\mathrm{S}[\mathrm{n}]|^2}$$

Adapting the corresponding values of LDACS1, the variance of the optimal estimator for the time shift τ can be obtained. With the propagation speed of electro-magnetic waves, denoted as c, the minimal mean range error $\bar{e}_{CRLB}$ is

$$\bar{e}_{CRLB} = \mathrm{c} \cdot \sqrt{VAR\{\hat{\tau}\}}.$$

Schmidl-Cox Coarse Synchronization Procedure

For coarse synchronization to the receive signal, a modified Schmidl-Cox algorithm is employed [11]. Its major advantage is that no pre-equalization of the channel has to be performed. Since the algorithm does not compare a stored sequence with a received one, but rather two received sequences with each other, it shows a low vulnerability towards fading radio channels.

The Schmidl-Cox algorithm exploits special properties of the synchronization sequences: in the first OFDM symbol only every fourth and in the second only every second sub-carrier is used. The use of the different sub-carriers is shown in Figure 3. The synchronization sequences in the frequency domain are given as

$$S_{\mathrm{sy},1}[n] = \sqrt{4} exp\left\{ j\pi \frac{5n^2}{N_{\mathrm{sy}1}} \right\}, \qquad n = 0, \dots, N_{\mathrm{sy}1} - 1$$

for the first and

$$S_{\mathrm{sy},2}[n] = \sqrt{2} exp\left\{ j\pi \frac{n^2}{N_{\mathrm{sy}2}} \right\}, \qquad n = 0, \dots, N_{\mathrm{sy}2} - 1$$

for the second OFDM symbol. Hereby $N_{\mathrm{sy}1}$ and $N_{\mathrm{sy}2}$ denote the number of used carriers in the first and second synchronization symbol, respectively. After the application of the IFFT, i.e. the conversion to the time domain, this leads to the signal structure shown in Figure 4.

The first symbol consists of four repetitions of the same signal part *B*, while the second symbol consists of two equal halves denoted as *A*. Furthermore, Figure 4 shows the position of the cyclic prefix CP, as well as the windowing part W.

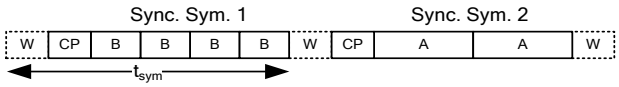

Figure 4. Structure of the Synchronization Symbols

The repetitive structure of the OFDM symbols can be exploited in order to find the start of a frame. A correlation function, further referred to as the synchronization metric, may be calculated. It compares the received values in a window with the received signal r in a shifted version of the same window at the instant d:

$$P[d] = \sum_{m=0}^{N_{\text{corr}}-1} r^*[d+m] \cdot r[d+m+N_{\text{diff}}]$$

The correlation length N_{corr} and the shift between the two correlation windows N_{diff} has to be adapted to the transmission parameters. For example for the second symbol the correlation length and shift are chosen as $N_{\text{corr}} = N_{\text{diff}} = N_{\text{FFT}}/2$. This leads to the second half of the OFDM symbol always being compared with its first half. Normalizing by the total energy in the window given as

$$N[d] = \frac{1}{2} \sum_{m=0}^{N_{\text{corr}}-1} (|r[d+m]^2| + |r[d+m+N_{\text{diff}}]^2|)$$

the metric M is calculated:

$$M[d] = \frac{|P[d]|^2}{(N[d])^2}$$

In M, calculated separately for the two synchronization symbols, the start of the frame is marked by a maximum. In the first metric additionally a maximum is found with a delay of one OFDM symbol. This can be useful if the original peaks for the start of the frame in the two metrics were not detected properly for some reason. Using the two metrics for the two synchronization symbols enables a rough determination of the starting point of the frame, even with noise and fading present.

An additional improvement may be obtained by also taking the cyclic prefixes of the OFDM symbols into account. This again translates into a repetition of the signal which can be exploited using the metric introduced above. Therefore N_{corr} is chosen as the cyclic prefix length and N_{diff} as the length of one OFDM symbol. In general the correlation of only one symbol's CP is significantly less reliable than taking the two synchronization symbols into account. However averaging the metric for all 26 OFDM symbols in a BC2 sub-frame increases the performance significantly. Thus, a correction for the first computation of the start of the frame using the two synchronization symbols can be calculated.

Time Domain Correlation With Low-pass Interpolation

As described above, the accuracy of the Schmidl-Cox algorithm, well sufficient for decoding of the received data, offers only restricted accuracy for determining the range to a ground station. Even with only little noise present, an error of one or few samples might occur. Using a realistic oversampling factor of 4, each sample has a duration of 0.4 µs equaling 120 m in distance error. Obviously this error cannot be tolerated for aeronautical positioning or ranging applications.

The second problem is that the algorithm does not offer a sub-sample resolution; the precision is always limited by the sampling rate. Although the oversampling rate may theoretically be increased to a factor offering a sufficient precision, this is not feasible for implementation into a real system.

In order to cope with the problems described above, two different approaches are studied offering both a higher precision as well as sub-sample resolution. The first approach evaluated is correlation in the time domain combined with ideal low pass interpolation: a metric m is calculated by correlating the receive signal $y[k]$ with the transmit signal $s[k]$

$$m[k] = y[k] * s[-k].$$

The $*$ denotes a discrete convolution. Hereby not all parts of the transmit signal may be known at the receiver. While knowledge for both the synchronization symbols and the pilots is always present at the receiver, the data symbols are not known a priori. Nevertheless, if the payload data is decoded, which under normal operational conditions should be possible, its integrity may be verified using the data's error detection checksum. The passing of that checksum, and therefore the assurance that the decoding of the data was successful, is very useful because of two reasons: Firstly, we know that the Schmidl-Cox algorithm detected the start of the frame with a precision sufficient for decoding the

data. This means, the distance to the ground station is already be known with a precision of a few kilometers. Otherwise decoding of the frame would not have been possible. Having this reliable starting point, the finer algorithms presented later in this paper, may be applied. Secondly, with being assured of the integrity of the payload, the data symbols may be used to increase the positioning performance.

The shift of the signal can be determined by looking at the maximum of the metric $m[k]$ introduced above. Note, that using this approach, the precision is limited by the sampling rate. However this problem may be solved by interpolation using the knowledge, that the underlying OFDM transmit signal is band limited.

In general, the signal $y(t)$ at the instant τ can be calculated from $y[k]$, if the band limited spectrum $S[n]$ is multiplied with the frequency response of the ideal low pass [12]. In the time domain this corresponds to a convolution with the $sinc$-function

$$s(\tau) = \sum_{k=-\infty}^{\infty} s[k] \cdot sinc(\pi \frac{\tau - kT_s}{T_s})$$

with T_s denoting the sampling duration of the signal.

The low pass interpolation is then applied on the calculation of the metric $m[k]$. Since both y[k] and s[k] and, therefore, also the correlation of both, the metric $m[k]$, are band limited, the metric at the time continuous instant τ, can be calculated as

$$m(\tau) = \sum_{k=-\infty}^{\infty} [s[\mathrm{k}] * y[\mathrm{k}]] \cdot sinc\left(\pi \frac{\tau - kT_s}{T_s}\right)$$

To find the maximum of the metric, the zeros of the first derivate $\frac{d}{d\tau} m(\tau)$ have to be found. As it can be seen from the formula above, the only term in $m(\tau)$ dependent on $\tau$is the $sinc$-function. Since it is an analytic function, the first and second order derivatives can be calculated as

$$\frac{d}{dx} sinc(x) = \frac{x\, cos(x) - \sin(x)}{x^2} \text{ and}$$
$$\frac{d^2}{dx^2} sinc(x) = \frac{(x^2 - 2)\, sin(x) + 2x \cos(x)}{x^3}.$$

The derivatives can now be used in a Newton's method finding the zeros of $\frac{d}{d\tau} m(\tau)$ and thus their local maximum. As a start value τ_0 the maximum of the discrete metric $m[k]$ is chosen. The following values in the iteration i are calculated as

$$\tau_{i+1} = \tau_i - \frac{\frac{d}{d\tau} m(\tau_i)}{\frac{d^2}{d\tau^2} m(\tau_i)}.$$

The procedure is repeated until a sufficiently accurate value is found.

Phase Analysis in Frequency Domain

In contrast to the algorithm above, which is performed in the time domain, the second approach is realized in the frequency domain. Again it is able to resolve the delay τ of the received signal on a sub-sample resolution. Note however, that a sufficiently accurate channel estimation and equalization for fading channels is required for proper functioning of the algorithm. Therefore, its implementation is generally more complex.

The algorithm exploits the fact, that a shift of the time domain signal *s(t)* corresponds to a phase rotation in the frequency domain of the signal *S(f)*

$$s(t - \tau) \Leftrightarrow S(f) \cdot e^{-j2\pi\tau}$$

Theoretically, this property can be used to determine the time shift with arbitrary precision. Therefore, the phases of both the discrete receive and transmit signal in the frequency domain, $S[n]$ and $Y[n]$, respectively, are calculated and subtracted from each other

$$\theta[n] = \varphi(S[n]) - \varphi(Y[n])\ mod\ 2\pi$$

Note that due to the $mod\ 2\pi$ term in the formula above, there is a phase ambiguity. Nevertheless this ambiguity relates to a distance of around 30 km and is therefore too large to cause any real problem. In general the shift calculated from the symbols on the sub-carriers with the indices n_1 and n_2, is given as

$$\hat{\tau} = \frac{64}{2\pi} \frac{\theta[n_2] - \theta[n_1]}{n_2 - n_1} T_s$$

with T_s being the duration of one base sample, i.e. 1.6 μs for LDACS1.

Using the formula above, under ideal conditions the shift, and therefore the range, can be exactly calculated. However, in any real scenario, there is noise present. To cope with that, a least-squares (LS) line is fitted through the vector of received

measurement points $\boldsymbol{\theta} = [\theta_1, \dots, \theta_N]^{\boldsymbol{T}}$. If the phase noise is modeled to be Gaussian, the LS-line and its slope $\hat{\tau}_{LS}$ is given as:

$$\begin{bmatrix} \hat{\tau}_{LS} \\ \tilde{c} \end{bmatrix} = \frac{64}{2\pi} T_s (\underline{\boldsymbol{X}}^T \underline{\boldsymbol{E}}^{-1} \underline{\boldsymbol{X}})^{-1} \underline{\boldsymbol{X}}^T \underline{\boldsymbol{E}}^{-1} \boldsymbol{\theta}$$

with $\underline{\boldsymbol{X}}$ being defined as the matrix of sub-carrier indices n_m, and $\underline{\boldsymbol{E}}$ the matrix with the symbol energies on the diagonal.

$$\underline{\boldsymbol{X}} = \begin{bmatrix} n[1] & 1 \\ \vdots & 1 \\ n[M] & 1 \end{bmatrix}; \quad \underline{\boldsymbol{E}} = \begin{bmatrix} E_1 & \cdots & 0 \\ \vdots & \ddots & \vdots \\ 0 & \cdots & E_M \end{bmatrix}$$

The second element $\tilde{c}$ of the result vector is a constant not relevant for the determination of the shift.

Simulation Results

This section deals with the results of the simulations performed to determine the ranging accuracy of the different algorithms described above. It starts with a short overview over the simulation system and its basic parameters. All results are compared with the corresponding CRLB.

For the range measurements only the LDACS1 BC2 frame is taken into consideration. Oversampling is set to a factor of four. This is a well established value for the LDACS1 communication system, but also turns out to offer good ranging performance for the coarse synchronization. Each frame is generated and a random shift of $\tau \in [0, T_s]$ is applied using ideal low pass interpolation. The random shift is assumed to be constant over the duration of one BC2. This is a realistic assumption since an aircraft at $250\,{}^{m}/_{s}$ cruise speed travels less than 1 m during one BC2 duration.

The signal is then passed through an AWGN channel, i.e. noise of the corresponding power is added. At the receiver in a first stage a coarse synchronization using the Schmidl-Cox like approach is conducted. This synchronization is only used for a rough determination of the start of the frame. Following that, the fine shifts are calculated for the two algorithms presented above, working in both the time and frequency domain. As described earlier, both algorithms can be applied on different sets of data, i.e. knowledge of the following transmit symbol groups can be assumed: synchronization sequences, data symbols, and pilot symbols. However, for the time domain correlation, the pilots and data symbols can only be taken into account jointly. This is due to the fact that the pilots are multiplexed with data symbols in the frequency domain. After the conversion to the time domain, both groups cannot be separated anymore easily for correlation. In order to be able to better evaluate the performance of the algorithms, the results are compared with the CRLB.

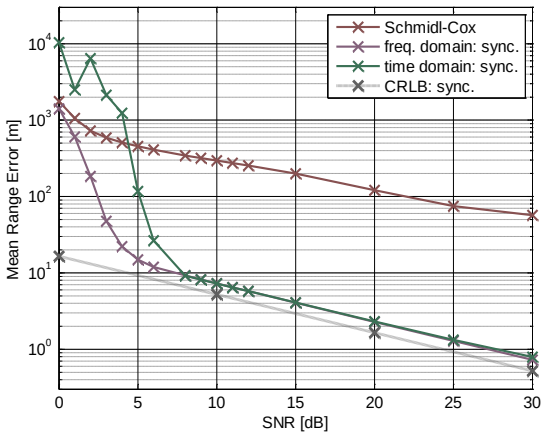

Figure 5. Mean Ranging Error (Synchronization Sequences Known at Receiver)

Figure 5 shows the results for the different algorithms, if only the synchronization symbols are taken into account. For a better comparison, also the corresponding CRLB is plotted. The results can be concluded as follows:

- In the lower SNR region, i.e. up to 5 dB, all algorithms offer a rather poor performance. While the coarse synchronization always stays well over a range error of 100 m, the two proposed algorithms approach the CRLB with increasing SNR. Whereas the frequency-domain approach converges quite rapidly, the time domain correlation exhibits ranging errors still above 100 m.
- For SNR above 5 dB, the coarse algorithm exhibits errors in the range of 100 times of those of the CRLB and, therefore, shows a rather poor performance. The two proposed algorithms show increasing accuracy with SNR almost meeting the CRLB for SNR values above 8 dB. For a

realistic SNR of 10 dB the average ranging errors for both algorithms are below 10 m.

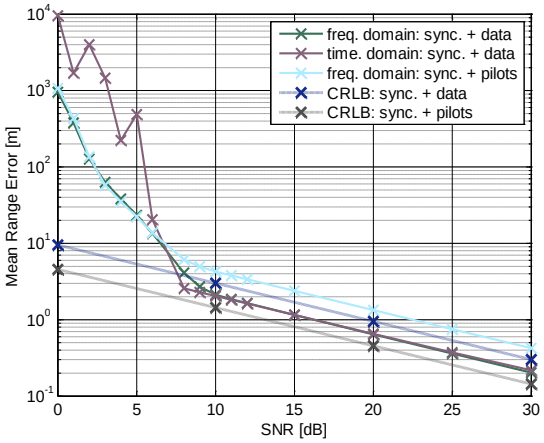

Figure 6. Mean Ranging Error (Data and Pilot Symbols Known at Receiver)

In Figure 6 the mean range errors are plotted for the scenario, where knowledge about pilot and data symbols is assumed. For the time domain approach only the case of using knowledge about both the pilots and data symbols jointly is considered, while in the frequency domain the pilots and data symbols can also be taken into account separately. For every simulation, the corresponding CRLB is plotted. The results can be concluded as follows:

- Both algorithms converge to the CRLB at an SNR of around 8 dB and are rather poor for lower SNR values. Similar to the results above, the time domain approach converges more slowly.
- For SNR above 8 dB both algorithms show a similar behavior with range errors close to the CRLB. For a realistic SNR of 10 dB, a mean range error of 2 m can be observed, if both data and pilot symbols are assumed to be known at the receiver. Considering only pilot and synchronization symbols leads to a mean accuracy of about 4 m.

Overall, the results show, that the two algorithms presented exhibit a “close to CRLB” ranging accuracy for an SNR above 8 dB. If it is assumed that the data symbols have been decoded correctly and are also used for determining the range, a performance of around two meters is well possible. For the lower SNR region the performance of all algorithms is mainly influenced by the occurrence of large, but rare errors. This is a very convenient error statistic, since the errors may easily be corrected by adequate filtering, e.g. a Kalman filter using a movement model of the aircraft. The application of such filters is planned for the future. This would most likely improve the performance significantly.

Another very interesting result is displayed in Figure 7. The plot shows the probability that the range error exceeds a certain value. For the creation of Figure 7 the time domain correlation algorithm at an SNR of 10 dB is employed. In the first curve only the synchronization sequence is assumed to be known at the receiver, while for the second the entire frame is considered for correlation.

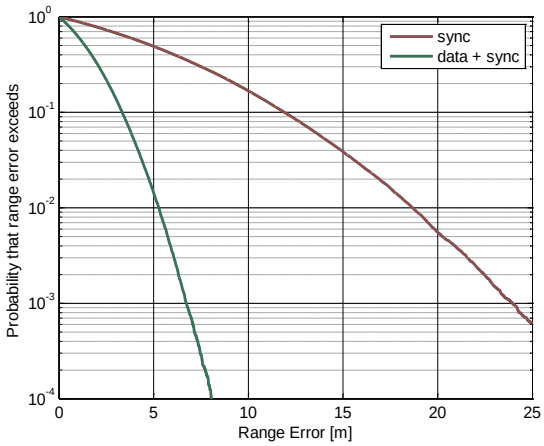

Figure 7. Error Distribution for the Time Domain Correlation

The results show that in both cases the probability for large errors decreases very quickly. If only the synchronization symbols are considered, less than 0.1 % of the errors exceed 24 m, while if the entire frame is taken into account, this value decreases to only 7 m. This again shows the potential of increasing the accuracy by application of a proper filtering.

Conclusions

In this paper, different ranging algorithms for navigation using LDACS1 are presented. The results show, that the original synchronization procedure, sufficient for communication, does not offer the

required accuracy for ranging or positioning applications. Nevertheless, at realistic SNR, the proposed algorithms in frequency and time domain offer accuracy close to the CRLB, meaning that the average errors are in the order of a few meters. In terms of ranging accuracy both algorithms only show differences for lower SNR regions where especially the time domain correlation shows low accuracy. Nevertheless, this small advantage of the frequency domain algorithm is most probably annihilated by its higher implementation complexity. Compared to the well-known DME system, independently from the algorithm employed, ranging with LDACS1 may offer an improvement in terms of accuracy by a factor of more than 10.

For the future, different options for research topics exist. Firstly, an extension from ranging to positioning is very preferable to allow evaluation of the expected navigation performance. Hereby of special interest is the combination with other sensors, e.g. barometer or inertial system. As mentioned above, another very promising approach is the adaption of a Kalman or similar filter to increase the accuracy of the ranging using a movement model of the aircraft. Additionally, of great interest is the examination of the ranging performance when a more realistic fading channel is employed for transmission.

In order to allow verification of the simulations a measurement campaign is currently prepared for fall 2012. It is planned to set up four LDACS1 GS on different ground locations allowing navigation of an aircraft flying over the set-up. The goal is to give a practical proof, that precise positioning using LDACS1 is possible in a realistic scenario.

References

[1] http://www.faa.gov/nextgen/

[2] http://www.sesarju.eu/

[3] http://www.eurocontrol.int/communications/public/standard_page/com_future.html

[4] A. H. Sayed, A. Tarighat, N. Khajehnouri, 2005; "Network-based wireless location: challenges faced in developing techniques for accurate wireless location information," *Signal Processing Magazine*

[5] C. Mensing, S. Plass, A. Dammann, 2007; "Synchronization Algorithms for Positioning with OFDM Communications Signals", *Positioning, Navigation and Communication (WPNC)*

[6] M. Schnell, U. Epple, F. Hoffmann, 2011; "Using the future L-band communication system for navigation", *Integrated Communications, Navigation and Surveilance Conference (ICNS)*, VA, USA

[7] M. Sajatovic, B. Haindl, M. Ehammer, Th. Gräupl, M. Schnell, U. Epple, S. Brandes, 2009; "LDACS1 System Definition Proposal: Deliverable D2", *Eurocontrol Study Report*, Edition 1.0.

[8] S. Brandes, U. Epple, M. Schnell, 2009; "Compensation of the Impact of Interference Mitigation by Pulse Blanking in OFDM Systems*"; Proceedings of IEEE Globecom*, HI, USA.

[9] N. Schneckenburger, N. Franzen, S. Gligorevic, M. Schnell, 2011; "L-band Compatibility of LDACS1"; *Digital Avionics Systems Conference (DASC)*, WA, USA

[10] Kay, M., 1993; "Fundamentals of Statistical Processing, Volume I"; *Prentice Hall*

[11] T. M Schmidl, D. C. Cox; "Robust frequency and timing synchronization for OFDM", *IEEE Transactions on Communications*, vol.45, no.12,

[12] R. Chrochiere, L. R. Rabiner, 1983; "Multirate Digital Signal processing"; *Prentice-Hall*